

Article

# Enhancing Wind Turbine Performance: Statistical Detection of Sensor Faults Based on Improved Dynamic Independent Component Analysis

K. Ramakrishna Kini <sup>1</sup>, Fouzi Harrou <sup>2,\*</sup>, Muddu Madakyaru <sup>3,\*</sup> and Ying Sun <sup>2</sup>

<sup>1</sup> Department of Instrumentation and Control Engineering, Manipal Institute of Technology, Manipal Academy of Higher Education, Manipal 576104, India; kr.kini@manipal.edu

<sup>2</sup> Computer, Electrical and Mathematical Sciences and Engineering (CEMSE) Division, King Abdullah University of Science and Technology (KAUST), Thuwal 23955-6900, Saudi Arabia; ying.sun@kaust.edu.sa

<sup>3</sup> Department of Chemical Engineering, Manipal Institute of Technology, Manipal Academy of Higher Education, Manipal 576104, India

\* Correspondence: fouzi.harrou@kaust.edu.sa (F.H.); muddu.m@manipal.edu (M.M.)

**Abstract:** Efficient detection of sensor faults in wind turbines is essential to ensure the reliable operation and performance of these renewable energy systems. This paper presents a novel semi-supervised data-based monitoring technique for fault detection in wind turbines using SCADA (supervisory control and data acquisition) data. Unlike supervised methods, the proposed approach does not require labeled data, making it cost-effective and practical for wind turbine monitoring. The technique builds upon the Independent Component Analysis (ICA) approach, effectively capturing non-Gaussian features. Specifically, a dynamic ICA (DICA) model is employed to account for the temporal dynamics and dependencies in the observed signals affected by sensor faults. The fault detection process integrates fault indicators based on  $I^2d$ ,  $I^2e$ , and squared prediction error (SPE), enabling the identification of different types of sensor faults. The fault indicators are combined with a Double Exponential Weighted Moving Average (DEWMA) chart, known for its superior performance in detecting faults with small magnitudes. Additionally, the approach incorporates kernel density estimation to establish nonparametric thresholds, increasing flexibility and adaptability to different data types. This study considers various types of sensor faults, including bias sensor faults, precision degradation faults, and freezing sensor faults, for evaluation. The results demonstrate that the proposed approach outperforms PCA and traditional ICA-based methods. It achieves a high detection rate, accurately identifying faults while reducing false alarms. It could be a promising technique for proactive maintenance, optimizing the performance and reliability of wind turbine systems.

**Keywords:** wind turbines; SCADA data; sensor faults; semi-supervised monitoring; data-driven methods; dynamic PCA; DEWMA



**Citation:** Kini, K.R.; Harrou, F.; Madakyaru, M.; Sun, Y. Enhancing Wind Turbine Performance: Statistical Detection of Sensor Faults Based on Improved Dynamic Independent Component Analysis. *Energies* **2023**, *16*, 5793. <https://doi.org/10.3390/en16155793>

Academic Editor: Davide Astolfi

Received: 11 June 2023

Revised: 31 July 2023

Accepted: 2 August 2023

Published: 4 August 2023



**Copyright:** © 2023 by the authors. Licensee MDPI, Basel, Switzerland. This article is an open access article distributed under the terms and conditions of the Creative Commons Attribution (CC BY) license (<https://creativecommons.org/licenses/by/4.0/>).

## 1. Introduction

Wind power has become an increasingly popular renewable energy source due to its numerous advantages. However, ensuring the reliability and availability of wind turbines is crucial to maximizing energy production and minimizing maintenance costs [1,2]. Wind power has numerous advantages over other forms of energy, making it an increasingly popular source of renewable energy worldwide. One of the key advantages of wind power is its ability to generate electricity without producing harmful greenhouse gas emissions, helping to mitigate climate change's impacts [3,4]. Additionally, wind power is a domestic energy source, reducing the dependence on foreign oil and improving energy security [5,6]. Wind turbines also have a relatively small land footprint compared to other forms of power generation, making them an attractive option for areas with limited available land. Wind turbines are becoming an increasingly popular renewable energy source due to their

ability to harness wind power and convert it into electricity [7]. As the number of wind turbines installed worldwide continues to rise, so does the need to ensure their reliable operation and maintenance [2]. One of the critical challenges in this regard is the detection of sensor faults that can cause a wide range of issues, including reduced energy production, equipment damage, and safety hazards.

Wind turbines are complex systems that require frequent maintenance to ensure optimal performance [8]. Fault detection is crucial to avoid costly downtime or equipment failure. Several methods for fault detection in wind turbines exist, including vibration analysis [9,10], acoustic monitoring [11,12], and temperature monitoring [13] (see Table 1). Vibration analysis involves measuring the vibrations of different components in the turbine to detect any anomalies that could indicate a fault. Acoustic monitoring uses microphones to pick up the sounds produced by the turbine, which can help identify issues such as blade damage or gearbox problems. Temperature monitoring involves measuring the temperature of various components in the turbine, such as the generator and gearbox, to detect any overheating that could indicate a fault. Advanced analytics and machine-learning algorithms can analyze the data collected from these methods to identify patterns or anomalies that could indicate a fault [14]. Early detection of faults using these methods can optimize wind turbine performance, reduce maintenance costs, and prevent costly downtime.

**Table 1.** Comparison of different fault detection approaches.

Approach	Advantages	Challenges
Vibration analysis	<ul style="list-style-type: none"> <li>• Can detect faults in various components</li> <li>• Provides detailed information</li> </ul>	<ul style="list-style-type: none"> <li>• Sensors can be expensive</li> <li>• Requires baseline measurement</li> <li>• Produces large amounts of data</li> </ul>
Acoustic monitoring	<ul style="list-style-type: none"> <li>• Can detect faults in the blades, gearbox, and bearings</li> <li>• Non-intrusive</li> <li>• Can detect faults at an early stage</li> </ul>	<ul style="list-style-type: none"> <li>• Requires specialized equipment</li> <li>• Wind turbine noise can be highly variable</li> <li>• Requires baseline measurement</li> </ul>
Temperature monitoring	<ul style="list-style-type: none"> <li>• Can detect faults in the generator, gearbox, and other components that generate heat</li> <li>• Relatively easy to perform</li> </ul>	<ul style="list-style-type: none"> <li>• Not always a reliable indicator of faults</li> <li>• Can produce false alarms</li> <li>• Cannot detect faults in non-heating components</li> </ul>

The SCADA (Supervisory Control and Data Acquisition) data are widely used to monitor wind turbine performance as it enables the detection of potential faults, leading to significant cost savings in maintenance and operation [15–17]. SCADA data provides a comprehensive view of the turbine’s performance and health compared to other monitoring methods such as vibration analysis, acoustic monitoring, and temperature monitoring. SCADA data offers real-time information on multiple turbine parameters, including rotor speed, blade pitch angle, generator output, and environmental conditions. By analyzing these data, operators can identify potential faults and performance issues early and optimize the turbine’s operation for maximum efficiency. In contrast, other monitoring methods may provide limited information on specific components or aspects of the turbine’s performance and may not detect certain faults or issues. Different techniques, such as data mining and control charts, can be applied to SCADA data to improve fault detection accuracy and identify the contributing variables [18,19].

Various data-based methods for enhancing fault detection in wind turbines based on SCADA data have been developed in the past two decades [20,21]. For instance, in [22], a PCA-based variable selection algorithm for condition monitoring of wind turbines is proposed. The algorithm uses multiple criteria to select variables that maximize dataset variability and contribute the most to a specific fault signal. Two fault diagnosis techniques

are proposed, one based on Hotelling  $T^2$  statistic for anomaly detection and the other for estimating fault severity using an empirical model. The algorithm is evaluated using SCADA data, and a dimension reduction of 45.5% is achieved while retaining variables with high cumulative percentage variance, percentage entropy, and low average correlation. The proposed algorithm can effectively diagnose fault signals with minimal loss of information. In one paper [23], a statistical data-driven modeling approach using multiway principal component analysis (MPCA) and multivariate inference is proposed for wind turbine condition monitoring based on SCADA data. The methodology is evaluated on a benchmark with a 5 MW high-fidelity wind turbine model and eight realistic fault scenarios, showing promising results for a wide range of significance levels. The use of multivariate hypothesis testing is shown to outperform the univariate case in terms of sensitivity, specificity, and false negatives. However, the study only considers faults related to mechanical components and does not consider other potential sources of faults, such as sensors. The study in [24] proposes a hybrid ReliefF-PCA-deep neural network (DNN) model for wind turbine fault diagnosis, which aims to reduce the dimensionality of the massive data generated during the operation of WTs and accurately diagnose the fault types and fault location. The ReliefF algorithm is used to extract sensitive fault features, while PCA is used to reduce the dimensions further and eliminate correlation among features.

Based on the feature subset, an optimized DNN is used to establish the fault diagnosis model. The proposed model achieves satisfactory accuracy in both single and multi-fault diagnoses. However, a limitation of this work is that the PCA method used to reduce dimensionality has limitations in handling non-linear and non-Gaussian data distributions. In one paper [25], Yang, et al. presented a fault detection technique that utilizes data mining to extract significant variables from SCADA data, followed by implementing a multivariate exponentially weighted moving average (MEWMA) model-based control chart. The method's effectiveness was evaluated using both SCADA data and alarm logs, and it was found that the MEWMA chart outperformed the single EWMA chart in fault detection. In another paper [26], an approach called fractional extended dispersion entropy (FrEDE) is proposed to detect faults in wind turbine systems. By integrating concepts from fractional calculus and dispersion entropy (DE), FrEDE enhances the utilization of information in raw signals and improves sensitivity to changes in complex wind turbines. The cumulative sum control chart (CUSUM) is adopted for monitoring the FrEDE series. This study highlights the potential of FrEDE as an effective tool for distinguishing normal from faulty states and detecting dynamic changes with low false alarm rates. In one paper [27], an approach based on canonical variate analysis (CVA) and partial least-squares regression (PLSR) is proposed to detect tricky faults in wind turbines. Specifically, the CVA-PLSR method maps the canonical variables to a new feature space using PLSR, which enhances the differences in statistics, particularly for tricky faults. Results through simulations on a wind turbine benchmark and real wind farm data sets showed that this approach outperformed three traditional methods, PCA, kernel canonical correlation analysis (KCCA), and CVA, in terms of accuracy.

In recent years, various machine-learning methods have been proposed for fault detection in wind turbines [28–31]. In [32], Zhang et al. introduced a data-driven approach that combines random forests (RFs) and extreme gradient boosting (XGBoost) algorithms to establish a fault detection framework. The approach entails conducting feature analysis to identify pertinent features for each specific fault, applying signal filtering, and utilizing RF-based feature ranking to select the most important features. The selected features are then used to train an XGBoost model, which constructs the fault detection classifiers. To evaluate the approach, numerical simulations are conducted using the advanced wind turbine simulator FAST, considering diverse wind turbine models and operating conditions. The results exhibit the approach's robustness across various wind turbine models, particularly in detecting sensor faults more effectively than actuator faults. In one paper [33], Xiang et al. propose a deep learning approach for fault detection in wind turbines using SCADA data analysis. The method combines convolutional neural network (CNN) and

long short-term memory network (LSTM) networks with an attention mechanism (AM) to improve learning accuracy. SCADA data are used as input, and the CNN captures dynamic changes in the data. The AM assigns weights to important information, enabling early warning for anomalies and predicting faulty components based on prediction residuals. Experimental results demonstrate the effectiveness of the method in detecting wind turbine failures. Other studies have investigated the application of the lightGBM algorithm [31], artificial neural networks [34], support vector machines [35], and ensemble learning [36] for fault detection in wind turbines.

The main contributions of this paper can be summarized as follows.

- This paper introduces a semi-supervised monitoring technique for fault detection in wind turbines utilizing SCADA data. The proposed approach does not need labeled data, relying solely on available fault-free SCADA data during model construction. As a result, it offers a cost-effective and efficient fault detection solution without requiring additional sensors or equipment installation.
- The second important contribution is the adoption of Independent ICA as a more effective approach for capturing non-Gaussian features in wind turbine data. By leveraging ICA's capability to represent original data in latent variables that are both non-Gaussian and independent, the proposed approach surpasses the performance of other semi-supervised schemes, including traditional methods like PCA [37,38]. Furthermore, to address the dynamic nature of wind turbine variables, the authors incorporated Dynamic ICA (DICA), which considers temporal dependencies and past information during the modeling stage. In addition, we enhanced the sensitivity of fault detection by integrating the fault indicators of ICA with a Double Exponential Weighted Moving Average (DEWMA) chart. Using DEWMA improves the detection of faults, particularly those with small magnitudes. Indeed, the DEWMA scheme incorporates information from past data in the decision process, making it more sensitive to small changes.
- The third significant contribution is the utilization of Kernel Density Estimation (KDE) to establish detection thresholds for the DICA-DEWMA detectors, introducing flexibility in the fault detection process. KDE enables the determination of appropriate thresholds for the DICA-DEWMA detectors in a non-parametric way, adapting to the specific characteristics of the wind turbine data and enhancing the accuracy of fault detection. Furthermore, the proposed approach has been comprehensively evaluated using various sensor faults, including precision degradation, freezing, and bias sensor faults. To quantify the detection performance, five statistical scores have been utilized. The evaluation results demonstrate the proposed approach's superior performance compared to conventional methods, such as PCA- and ICA-based techniques. This highlights the promising potential of the proposed approach in detecting and identifying different sensor fault types in wind turbines.

We organize the whole paper in the following manner: Section 2 presents an overview of the Independent Component Analysis (ICA), the Dynamic ICA (DICA) modeling approach, and the Double Exponential Weighted Moving Average (DEWMA) chart. It also outlines the block diagram representation of the proposed DICA-DEWMA semi-supervised FD technique. In Section 3, the performance of the proposed FD strategy is validated using different sensor faults on a wind turbine data set. Finally, Section 4 concludes the paper with a summary of the findings and also discusses the potential future research directions.

## 2. Methodology

This section provides an overview of the ICA-based FD scheme, the DICA-based FD scheme, the DEWMA chart, and the proposed DICA-DEWMA strategy. These components form the foundation of the proposed fault detection technique and contribute to the effectiveness and reliability of fault detection in wind turbines.

### 2.1. Independent Component Analysis

Independent Component Analysis (ICA) is a statistical technique that separates a set of mixed signals into their underlying independent components. It is a powerful method that can uncover the hidden structure and underlying data sources by assuming that the observed signals are linear mixtures of these sources. Essentially, the fundamental principle of ICA is transforming the observed signals into a new set of statistically independent variables. This transformation is achieved by finding a linear matrix that maximizes the independence between the components. In other words, the goal of ICA is to find a representation of the data where the components are as statistically independent as possible. One of the key advantages of ICA is its ability to model non-Gaussian data. Unlike other linear transformation techniques, such as Principal Component Analysis (PCA), which assumes that the components are Gaussian, ICA does not make any distributional assumptions [39]. This flexibility enables ICA to handle real-world data exhibiting non-Gaussian variations and complex dependencies. In the context of fault detection in wind turbines, ICA can be applied to extract the underlying fault signatures or patterns from the observed signals. By separating the normal operating behavior from the fault-related components, it becomes possible to detect and identify the presence of faults in the system.

ICA is a powerful multivariate method that aims to maximize the independence of latent variables, known as independent components (ICs) [38]. Unlike other linear transformation techniques, ICA utilizes higher-order statistics, such as negentropy or kurtosis, to represent data. Given a dataset consisting of variables  $x_1, x_2, \dots, x_m$ , ICA seeks to decompose it into a combination of  $l$  (where  $l \leq m$ ) unknown ICs, denoted as  $s_1, s_2, \dots, s_l$ . The relationship between the data and ICs can be described as follows [40]:

$$\mathbf{X} = \mathbf{A}\mathbf{S} + \mathbf{E}. \quad (1)$$

In Equation (1), the matrix  $\mathbf{S}=[s_1, s_2 \dots s_n] \in \mathfrak{R}^{l \times n}$  represents the matrix of independent components (ICs), where  $s_1, s_2, \dots, s_n$  are the individual ICs. The matrix  $\mathbf{A}=[a_1 \dots a_l] \in \mathfrak{R}^{m \times l}$  is the unknown mixing matrix, and  $\mathbf{E} \in \mathfrak{R}^{m \times n}$  denotes the residual matrix. The de-mixing matrix  $\mathbf{W}$  is then calculated based on the estimated IC matrix  $\hat{\mathbf{S}}$  as follows:

$$\hat{\mathbf{S}} = \mathbf{W}\mathbf{X}. \quad (2)$$

After data pre-processing, the next step is the whitening process, which aims to eliminate correlations present in the data variables. The whitening transformation is defined as  $\mathbf{Z} = \mathbf{Q}\mathbf{X}$ , where  $\mathbf{Q} = \mathbf{\Gamma}^{-1} \mathbf{U}^T$ ,  $\mathbf{\Gamma}$  is a matrix with the diagonal eigenvalues, and  $\mathbf{U}$  is a matrix containing the eigenvectors obtained from the covariance of  $\mathbf{X}$ . The resulting transformation after whitening can be represented as follows [41]:

$$\mathbf{Z} = \mathbf{Q}\mathbf{X} = \mathbf{Q}\mathbf{A}\mathbf{S} = \mathbf{B}\mathbf{S}. \quad (3)$$

Using the information from Equation (3), the estimation of  $\mathbf{S}$  can be expressed as follows:

$$\hat{\mathbf{S}} = \mathbf{B}^T \mathbf{Z} = \mathbf{B}^T \mathbf{Q}\mathbf{X}. \quad (4)$$

Using the information from Equations (2) and (4), a relationship between  $\mathbf{W}$  and  $\mathbf{B}$  can be established as follows:

$$\mathbf{W} = \mathbf{B}^T \mathbf{Q}. \quad (5)$$

To compute  $\mathbf{B}$ , each column vector  $\mathbf{b}_i$  is assigned an initial value and then updated iteratively using an algorithm that maximizes non-gaussianity based on Negentropy approximation [42]. This iterative process aims to estimate the independent components (ICs) by iteratively refining the values of  $\mathbf{B}$ .

The fixed-point algorithm used to determine the ICs can be described by the following steps:

1. Select a total of  $p$  ICs to be computed and initialize the counter as  $k = 1$ .

2. Set the initial value of the matrix  $\mathbf{B}$  as an identity matrix of size  $m \times m$ .
3. Compute  $b_k$  using the equation:  $b_k \leftarrow \text{Ezg}(b_k^T z) - \text{Eg}'(b_k^T z)b_k$ , where  $g$  and  $g'$  represent the first and second derivatives of the quadratic function  $G$ , respectively.
4. Perform deflationary orthogonalization: Update  $b_k$  as  $b_k \leftarrow b_k \leftarrow \sum_{k=1}^{k-1} (b_k^T b_k) b_k$  and normalize  $b_k$  as  $b_k \leftarrow \frac{b_k}{\|b_k\|}$ .
5. Check if  $b_k$  has converged to the value of the previous iteration. If it has, output  $b_k$ . If  $k \leq l$ , increment the value of  $k$  by 1 and return to step 1.

Once the ICs are computed using the iterative algorithm, the next task is to select the optimal ICs. This is achieved by utilizing the cumulative percentage variance (CPV) scheme. The CPV scheme allows us to determine the number of significant ICs that capture the majority of the variation in the data. To implement the CPV scheme, the eigenvalues corresponding to each IC are sorted in descending order. The cumulative sum of these eigenvalues is then computed, and the percentage of the total sum of eigenvalues is calculated for each IC. By analyzing the CPV curve, one can identify the point at which the curve begins to plateau, indicating diminishing returns in terms of capturing additional variance. The optimum number of ICs is determined by selecting a threshold value on the CPV curve, representing the desired variance level to be retained. Typically, a threshold of 90% or higher is chosen to ensure that a significant portion of the variance is accounted for. The ICs corresponding to the selected eigenvalues are then retained for further analysis and interpretation. By employing the CPV scheme, we can effectively identify the most informative and influential ICs that contribute significantly to the overall variation in the data, enabling a more concise and meaningful representation of the underlying processes.

Once an ICA model is constructed, it can be utilized to monitor abnormalities in new data by employing three key statistics:  $I_d^2$ ,  $I_e^2$ , and squared prediction error (SPE). These statistics play a crucial role in detecting deviations from the expected behavior and identifying potential faults.  $I_d^2$  measures the contribution of each IC to the overall data variation. It quantifies the relevance of an IC in explaining the observed data and serves as an indicator of its abnormality. A higher value of  $I_d^2$  suggests a stronger contribution of the corresponding IC to the observed anomalies. The  $I_e^2$  index assesses each IC's contribution to the original data's estimation. It evaluates the extent to which an IC captures the important information in the observed data. Higher values of  $I_e^2$  indicate greater relevance and usefulness of the IC in estimating the original signals. The SPE evaluates the discrepancy between the reconstructed data using a subset of ICs and the original data. It quantifies the model's prediction accuracy and serves as a measure of the model's performance. A higher SPE value indicates a larger discrepancy between the reconstructed and original data, suggesting potential anomalies. The three monitoring statistics, namely  $I_d^2$ ,  $I_e^2$ , and SPE, are defined as follows:

$$I_d^2(i) = \mathbf{f}_{new\ l}^T(i) \mathbf{f}_{new\ d}(i), \quad (6)$$

$$I_e^2(i) = \mathbf{f}_{new\ m-l}^T(i) \mathbf{f}_{new\ m-l}(i), \quad (7)$$

$$SPE(i) = (\mathbf{X}_{new}(i) - \hat{\mathbf{X}}_{new}(i))^T (\mathbf{X}_{new}(i) - \hat{\mathbf{X}}_{new}(i)), \quad (8)$$

where where  $\mathbf{f}_{new\ l} = \mathbf{W}_l \mathbf{X}_{new\ l}$ ,  $\mathbf{f}_{new\ m-l} = \mathbf{W}_{m-l} \mathbf{X}_{new\ m-l}$  are computed for a new data  $\mathbf{X}_{new}$  with  $\mathbf{W}_l$  is a matrix obtained by selection of  $l$  rows,  $\mathbf{W}_{m-l}$  is a matrix obtained by selection of excluded  $m-l$  rows of the separating matrix  $\mathbf{W}$ ,  $\hat{\mathbf{X}}_{new} = \mathbf{Q}^{-1} \mathbf{B}_l \hat{\mathbf{s}}_{new}(i) = \mathbf{Q}^{-1} \mathbf{B}_l \mathbf{W}_l \mathbf{X}_{new}(i)$  [38].

Please note that in its traditional form, ICA is a static model that focuses on the statistical independence of the source signals in the observed mixed signals. It does not inherently incorporate information from past data or explicitly model temporal dynamics. To handle temporal dynamics and incorporate temporal information, researchers have developed extensions of ICA known as Dynamic ICA or time-dependent ICA. Dynamic ICA is an extension of traditional ICA that aims to handle temporal dynamics, incorporate informa-

tion from past data, and model the temporal dependencies in the observed signals. These approaches provide a way to analyze time-varying signals and capture the underlying dynamics in the data.

## 2.2. Dynamic ICA

In industrial settings, the variables and measurements are often correlated over time due to the inherent dynamics of the underlying processes. Additionally, these variables are subject to various noise sources, disturbances, and uncertainties, preventing them from staying in a steady state condition [41]. While the static ICA fault detection strategy has shown promising performance, it fails to capture the temporal correlations among the variables. To enhance the monitoring capability, it is necessary to incorporate the system's dynamics during the modeling stage before developing the fault detection scheme. To address this issue, a Dynamic ICA (DICA)-based scheme is employed, which allows for the inclusion of time-lagged variables in the original ICA matrix. By augmenting each variable with past observations, a new matrix is constructed that accounts for the temporal dependencies within the data [42,43]. This incorporation of lagged variables captures the dynamic behavior of the system and enables a more accurate representation of the underlying processes. Importantly, by integrating the temporal dynamics into the fault detection model, the proposed DICA-based scheme offers improved performance in monitoring industrial systems. It enables the detection of faults and abnormalities that static approaches may not capture. Including lagged variables in the ICA matrix provides a more comprehensive understanding of the system behavior and enhances the sensitivity of the fault detection scheme to deviations from normal operation [42,44]. The augmented data matrix can be computed as [43]:

$$\mathbf{X}(l) = \begin{bmatrix} \mathbf{x}_t^T & \mathbf{x}_{t-1}^T & \cdots & \cdots & \mathbf{x}_{t-l}^T \\ \mathbf{x}_{t-1}^T & \mathbf{x}_{t-2}^T & \cdots & \cdots & \mathbf{x}_{t-1-l}^T \\ \cdot & \cdot & \cdot & \cdot & \cdot \\ \cdot & \cdot & \cdot & \cdot & \cdot \\ \cdot & \cdot & \cdot & \cdot & \cdot \\ \mathbf{x}_{t+l-n}^T & \mathbf{x}_{t+l-n-1}^T & \cdots & \cdots & \mathbf{x}_{t-n}^T \end{bmatrix}, \quad (9)$$

Here, the observations are represented by the observation vector  $\mathbf{x}_t^T$  at each time instant  $t$ . The number of observations is denoted by  $n$ , and the parameter  $l$  corresponds to the number of lagged measurements [41]. By applying static ICA to the constructed matrix, a dynamic ICA fault detection strategy is obtained. To capture the dynamic and static behavior of process variables, it is crucial to select an appropriate value for the time lag, denoted as  $l$ . Based on empirical analysis, it has been observed that using a small number of lags, such as  $l = 1$  or  $l = 2$ , yields satisfactory results for the DICA-based fault detection strategy [45]. Therefore, this study considers a lag of either  $l = 1$  or  $l = 2$  for the DICA modeling and subsequent fault detection analysis. This choice allows for the incorporation of relevant temporal information while maintaining computational efficiency.

## 2.3. Double EWMA Scheme

The DEWMA scheme was designed to enhance the detection of small changes in the process mean. A comparative study conducted in [46] demonstrated that the DEWMA scheme outperforms the traditional single EWMA scheme in detecting such small changes. However, for moderate and large faults, both techniques showed comparable performance. The DEWMA charting statistic, denoted as  $w_t$ , is computed as follows:

$$\begin{cases} w_0 = s_0 = \mu_0, \\ w_t = \nu s_t + (1 - \nu) w_{t-1}, \\ s_t = \nu x_t + (1 - \nu) s_{t-1}, \quad t = 1, 2, \dots, n. \end{cases} \quad (10)$$

In Equation (10),  $\mu_0$  represents the mean value in the absence of anomalies, and  $\nu$  denotes the smoothing parameter, which takes a value between 0 and 1. Please note that the DEWMA scheme, which employs two different smoothing parameters to compute the statistics  $w_t$  and  $s_t$  in Equation (10), has been found to exhibit comparable performance to the DEWMA scheme with equal parameters, as demonstrated in [46]. In this work, we have adopted the DEWMA scheme with equal smoothing constants, as recommended by Zhang and Chen (2005) [46].

In the traditional DEWMA chart, the detection thresholds are computed based on the assumption of Gaussian-distributed data. However, in practical applications, the assumption of Gaussian distribution may not always hold true for the data. Real-world data often exhibit non-Gaussian characteristics, such as heavy tails or skewness, which can significantly impact the accuracy of the detection thresholds [47]. Therefore, relying solely on Gaussian assumptions may lead to suboptimal performance in detecting anomalies. To address this limitation, alternative approaches are needed to compute detection thresholds that are more robust to the non-Gaussian nature of the data. One such approach is to utilize non-parametric techniques, such as the Kernel Density Estimation (KDE), to estimate the underlying probability distribution of the charting statistics. By employing KDE, the detection thresholds can be determined based on the estimated distribution of the charting statistics without making restrictive assumptions about the data distribution. The use of non-parametric methods, such as KDE, offers increased flexibility and adaptability to the specific characteristics of the data. This approach allows for a more accurate representation of the data distribution, considering its non-Gaussian properties. Consequently, the detection thresholds derived from the estimated distribution are better tailored to the actual data characteristics, enhancing the sensitivity and specificity of the DEWMA chart in practical applications. By considering the non-Gaussian nature of the data and employing non-parametric techniques for threshold computation, the proposed approach provides a more robust and reliable method for anomaly detection in real-world scenarios. It enables the detection of anomalies even in situations where the data deviate significantly from Gaussian assumptions, thus enhancing the overall effectiveness of the DEWMA chart in practical applications.

### 3. The Proposed Detection Approach

The proposed fault detection strategy aims to enhance the capability of detecting faults in multivariate processes by integrating two powerful techniques: the DICA strategy and the DEWMA chart. This integration aims to address two important aspects of fault detection: capturing the dynamics of process variables and detecting small variations in their behavior.

The initial step in the strategy involves the DICA scheme, which leverages the ability of ICA to capture non-Gaussian features in the process data. However, it recognizes that process variables often exhibit strong dynamics, which can significantly impact their behavior. To account for this, the Dynamic ICA scheme introduces lags in the modeling stage. By considering lagged measurements, it incorporates the temporal dependencies and captures the dynamic behavior of the variables more accurately. To further enhance the sensitivity of fault detection, the DEWMA scheme is incorporated into the strategy. The DEWMA is known for its effectiveness in detecting small changes in the process mean. Overall, the proposed DICA-DEWMA-based fault detection strategy combines the strengths of DICA and DEWMA to provide an enhanced approach for detecting faults in industrial processes.

Figure 1 depicts the sequential steps of the proposed DICA-DEWMA-based fault detection strategy. The figure serves as an informative visual aid for readers to understand the methodology and the key components of the proposed fault detection framework. The diagram illustrates two stages: offline training (model development) and online testing (online monitoring). During the offline training stage, the strategy learns from historical data to establish the necessary models and parameters. This stage involves three crucial

steps: data preprocessing, DICA modeling with lagged variables, and computation of the DEWMA detection threshold. The raw data are prepared and preprocessed in the data preprocessing step to ensure their suitability for subsequent analysis. The DICA modeling with lagged variables enables the capture of temporal dependencies and past information in the wind turbine data, considering its dynamic nature. Subsequently, the DEWMA detection threshold is computed to enhance the sensitivity of fault detection, particularly for detecting faults with small magnitudes. Once the offline training stage is completed, the strategy transitions to the online testing stage, where it applies the learned models and parameters to monitor real-time data and detect any potential faults in the wind turbine system. In the online testing stage, monitoring statistics are computed based on the incoming data, and these statistics are then compared with predefined thresholds established during the offline training stage. This threshold comparison enables the strategy to make informed decisions and detect any deviations or abnormalities in the system's behavior.

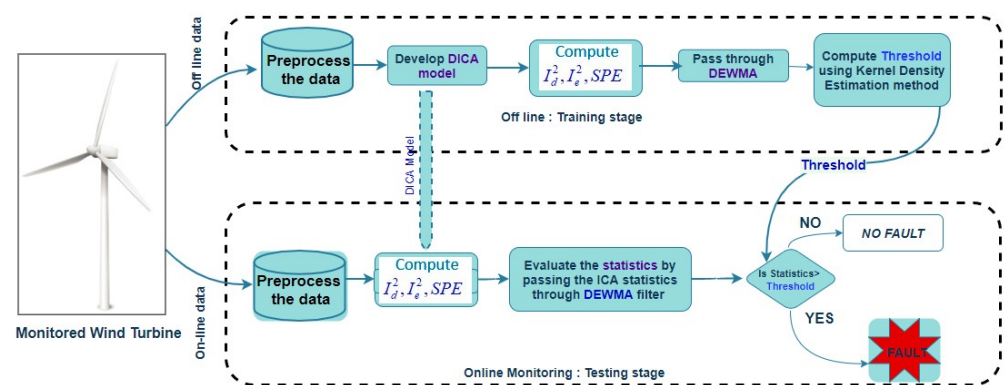


**Figure 1.** Proposed DICA-DEWMA-based Fault detection strategy.

The offline training stage comprises the following steps:

- (1) Pre-processing of the training data obtained from the wind turbine set-up, which is free from anomalies or faults.
- (2) Computation of the optimal number of lags to capture the dynamics of the variables, followed by the construction of the DICA model with the lagged variables.
- (3) Computation of thresholds for three fault indicators, namely DEWMA- $I^2d$ , DEWMA- $I^2e$ , and DEWMA-SPE, using the KDE approach. These thresholds will be used to determine the presence of faults during the online testing stage.

The online testing stage includes the following steps:

- (1) Pre-processing the new online data obtained from the inspected wind turbine.
- (2) Augmentation of the testing data with the appropriate lagged variables, considering the dynamic nature of the process.
- (3) Computation of the fault indicators  $I^2d$ ,  $I^2e$ , and SPE based on the augmented testing data.
- (4) Calculation of the DEWMA statistic based on the computed fault indicators (i.e.,  $I^2d$ ,  $I^2e$ , and SPE) obtained in the previous step.
- (5) Comparison of the calculated statistics with the reference threshold values established during the offline training stage. If the statistical indicators fall within the threshold range, the process is operating normally and free from faults. If the statistical indicators exceed the threshold values, it indicates the presence of a fault or anomaly in the process.

In the proposed fault detection strategy, it is recognized that wind turbine process variables often deviate from a Gaussian distribution. Therefore, the traditional approach of computing thresholds based on Gaussian assumptions may not be effective and can lead to increased missed detections and false alarms. The proposed method employs the Kernel Density Estimation (KDE) approach to determine the threshold for DEWMA-based

detectors using anomaly-free data, providing enhanced flexibility. The Probability Density Function (PDF) of the charting statistics is estimated using the KDE technique, allowing for a more accurate representation of the underlying distribution. The KDE approach utilizes a kernel estimator  $K$ , which is a smoothing function centered around each data point. The estimator calculates the contribution of each observation value  $z_j$  to the density estimation at a specific data point  $z$ . By considering the contributions of all observations in the dataset, the KDE provides an estimate of the underlying distribution of the data [48]. The kernel estimator  $K$  is defined as follows:

$$\hat{f}_z = \frac{1}{nh} \sum_j 1^n K\left(\frac{z - z_j}{h}\right). \quad (11)$$

The KDE approach requires the specification of a smoothing parameter  $h$ . This parameter controls the kernel function's bandwidth and determines the estimated density's smoothness. A smaller  $h$  value results in a narrower kernel and a more localized estimate, while a larger  $h$  value leads to a broader kernel and a smoother estimate. This algorithm has been extensively employed across various domains, encompassing diverse applications, such as outlier detection and fault detection [49,50].

To determine the threshold for the fault indicators ( $I^2d$ ,  $I^2e$ , and SPE), the KDE is applied to the anomaly-free training data. The KDE estimates the probability density function of each indicator, capturing the non-Gaussian characteristics of the variables. The detection threshold is then determined based on the estimated distribution of charting statistics, specifically the  $(1 - \alpha)$ -th quantile, where  $\alpha$  is a predefined significance level. This approach enables the identification of anomalies by comparing the DEWMA charting statistics against the established threshold. The proposed fault detection strategy offers increased flexibility and accuracy in determining the thresholds for detecting faults by employing the KDE-based approach. It considers the non-Gaussian nature of the process variables and provides a more reliable control limit based on the estimated distribution of the fault indicators.

## 4. Results and Discussion

### 4.1. Data Description

This study utilizes the SCADA dataset obtained from a Senvion MM82 wind turbine located in France. Further information regarding the key features of this specific wind turbine can be found in [14]. The data were gathered throughout 2017 at ten-minute intervals. The collected variables and their corresponding units of measurement are provided in Table 2.

Table 3 presents a statistical summary of the measured variables in the training SCADA data. These statistics provide valuable insights into the distribution and characteristics of the variables. These statistical descriptors provide a comprehensive overview of the characteristics of the measured variables, offering insights into their range, variability, central tendency, skewness, and kurtosis. Skewness measures the asymmetry of the distribution. Positive skewness indicates a longer right tail, while negative skewness indicates a longer left tail. For example, the variable  $P$  has a skewness of 1.21, suggesting a slightly right-skewed distribution. Kurtosis measures the peakedness or flatness of the distribution compared to a normal distribution. Positive kurtosis indicates a more peaked distribution, while negative kurtosis indicates a flatter distribution. For instance, the variable  $P$  has a kurtosis of 3.34, indicating a moderately peaked distribution.

The datasets collected in this study exhibit non-Gaussian distribution characteristics (Table 3). This non-Gaussian behavior of the data poses a challenge for fault detection approaches that are designed based on the assumption of Gaussian process variables. As wind turbine data are non-Gaussian, ICA holds promise in this context by appropriately capturing its non-Gaussian features, leading to a more precise representation of the underlying process dynamics.

**Table 2.** SCADA wind turbine measurements.

Variable	Description
P	Active power (kW)
Ds	Generator speed (rpm)
Db1t	Generator bearing 1 temperature (°C)
Db2t	Generator bearing 2 temperature (°C)
Dst	Generator stator temperature (°C)
Gb1t	Gearbox bearing 1 temperature (°C)
Gb2t	Gearbox bearing 2 temperature (°C)
Git	Gearbox inlet temperature (°C)
Gost	Gearbox oil sump temperature (°C)
Ya	Nacelle angle (°)
Yt	Nacelle temperature (°C)
Ws1	Wind speed (m/s). First anemometer on the nacelle
Ws2	Wind speed (m/s). Second anemometer on the nacelle
Ws	Average wind speed (m/s)
Wa	Absolute wind direction (°)
Ot	Outdoor temperature (°C)
Rbt	Rotor bearing temperature (°C)

**Table 3.** Statistical Summary of the training SCADA data.

Variables	Min	Max	STD	Q1	Median	Q3	Skewness	Kurtosis
P	−414.32	2489.27	803.01	143.79	525.03	1619.66	0.54	1.77
Ds	−267.00	2200.13	581.10	1111.10	1604.69	1816.19	−1.21	3.45
Db1t	7.35	51.94	7.33	33.26	38.90	43.34	−0.84	4.03
Db2t	5.50	44.39	5.22	32.25	35.21	37.72	−1.96	9.52
Dst	7.58	84.56	9.92	56.46	60.64	64.32	−2.26	9.99
Gb1t	12.51	80.36	10.95	60.04	66.42	70.67	−1.74	6.40
Gb2t	13.87	82.25	11.48	59.32	68.26	72.56	−1.50	5.13
Git	16.24	62.75	6.42	51.54	54.14	56.13	−2.41	10.13
Gost	18.87	70.42	7.12	55.17	58.06	60.02	−2.12	8.45
Ya	−26.96	387.38	85.49	118.37	202.43	248.53	−0.36	2.28
Yt	4.18	32.53	5.63	16.42	22.07	25.35	−0.44	2.21
Ws1	−1.68	33.18	4.49	6.17	8.53	12.39	0.41	3.07
Ws2	−1.53	32.15	4.17	6.01	8.30	11.83	0.45	3.07
Ws	−1.46	31.46	4.31	6.02	8.30	11.92	0.46	3.09
Wa	−32.89	386.73	89.02	137.51	231.34	278.39	−0.52	2.36
Ot	−2.07	19.87	3.67	4.59	6.90	9.53	0.25	3.07
Rbt	8.04	29.83	3.52	22.23	24.40	25.95	−1.42	5.26

#### 4.2. Fault Detection Results

In this section, we aim to assess and compare the performance of the ICA Double EWMA-based indicators on various types of faults in the wind turbine process. We evaluate the effectiveness of the following schemes: DICA-DEWMA- $I^2d$ , DICA-DEWMA- $I^2e$ , and DICA-DEWMA-SPE. To establish a baseline for comparison, we also consider other fault detection schemes, namely PCA- $T^2$ , PCA-SPE, PCA- $T^2$ -DEWMA, PCA-SPE-DEWMA, DPCA- $T^2$ , DPCA-SPE, DPCA- $T^2$ -DEWMA, DPCA-SPE-DEWMA, ICA- $I^2d$ , ICA- $I^2e$ , ICA-SPE, ICA-DEWMA- $I^2d$ , ICA-DEWMA- $I^2e$ , ICA-DEWMA-SPE, DICA- $I^2d$ , DICA- $I^2e$ , and DICA-SPE. Here, PCA- $T^2$  and PCA-SPE schemes are considered baseline models due to their widespread use in fault detection applications [51]. The PCA- $T^2$  scheme monitors change in the principal components subspace, while the PCA-SPE scheme monitors the residual subspace. Based on PCA, these methods are well-established and commonly employed as benchmarks for comparison in fault detection studies.

SCADA data contain vital information about a wind turbine's operational and performance status. In this study, we utilize a dataset comprising 6000 data points for the model development stage. Additionally, we use 4000 data points to validate the proposed

approach. The training data are collected over a specific period, ranging from 1 February 2017 to 14 March 2017. During this period, the historical SCADA data are employed to establish the necessary models and parameters for our fault detection approach. Subsequently, the testing data are recorded from 14 March 2017 to 11 April 2017. This dataset represents real-time SCADA data, which are used to evaluate the performance of the proposed approach in detecting and identifying various sensor fault types in wind turbines. By utilizing these distinct datasets for model development and validation, we ensure a rigorous and accurate assessment of the proposed DICA-DEWMA-based fault detection strategy. The PCA and ICA models are constructed using the training data, retaining nine Principal Components (PCs) and Independent Components (ICs). Similarly, the DPCA and DICA models are constructed using the training data, retaining 17 PCs and 17 ICs, respectively, employing the Cumulative Proportion of Variance (CPV) approach.

By contrasting the performance of these schemes against each other, we can gain insights into their effectiveness in detecting various types of faults in the wind turbine process. This evaluation allows us to identify the most robust and accurate fault detection strategy for wind turbine monitoring.

The proposed fault detection strategy will undergo evaluation using a set of simulated sensor faults. In real-world scenarios, recorded sensor data can be corrupted due to various types of sensor faults, including bias, drift, loss of accuracy, and degradation. In this study, we simulate these faults by introducing specific sensor faults, such as bias, drift, intermittent, freezing, and precision degradation. By introducing these simulated faults, we create scenarios where the faults are known, allowing for a systematic assessment of the different strategies. A summary of the fault scenarios considered in this study is presented in Table 4. By evaluating the proposed strategy against these simulated fault scenarios, we can gain insights into its performance and compare it with other strategies.

**Table 4.** Considered sensor faults in this study.

Fault	Description	Variable	Type
F1	Step (15% of total variation)	Gb2t	Bias sensor fault
F2	Ramp (Slope of 1)	Db1t	Precision Degradation fault
F3	Stuck at 77.7 degree	Ws1	Freeze sensor fault
F4	Ramp with noise (Slope of 0.03)	Ds	Bias sensor fault
F5	Multiple (12% of total variation)	Ds	Precision Degradation fault

The detection performance of the proposed fault detection strategy was assessed using various evaluation metrics, including False Positive Rate (FPR), True Positive Rate (TPR), Precision, Recall, and F1-score. The FPR measures the ratio of falsely detected faults to the total number of fault-free instances. It indicates the strategy's ability to avoid false alarms and maintain a low rate of false positives.

$$FPR = \frac{\text{False Positives}}{\text{False Positives} + \text{True Negatives}} \quad (12)$$

The TPR, also known as sensitivity or recall, quantifies the proportion of actual faults that are correctly identified by the detection strategy. A high TPR indicates the strategy's effectiveness in capturing and detecting real faults.

$$TPR = \frac{\text{True Positives}}{\text{True Positives} + \text{False Negatives}} \quad (13)$$

Precision measures the proportion of correctly identified faults out of all the instances identified as faults by the strategy. It reflects the strategy's accuracy in correctly labeling true positives and avoiding false positives.

$$\text{Precision} = \frac{\text{True Positives}}{\text{True Positives} + \text{False Positives}}. \quad (14)$$

Recall, also referred to as sensitivity, is synonymous with the TPR. It represents the proportion of actual faults that are correctly detected by the strategy.

$$\text{Recall} = \frac{\text{True Positives}}{\text{True Positives} + \text{False Negatives}}. \quad (15)$$

The F1-score combines precision and recall into a single metric that provides a balanced assessment of the detection strategy's performance. It is the harmonic mean of precision and recall, providing a comprehensive evaluation of the strategy's effectiveness in identifying faults while minimizing false positives.

$$\text{F1-score} = 2 \times \frac{\text{Precision} \times \text{Recall}}{\text{Precision} + \text{Recall}}. \quad (16)$$

By evaluating the strategy using these metrics, we can comprehensively understand its detection performance, including its ability to accurately detect faults, avoid false alarms, and strike a balance between precision and recall.

#### 4.2.1. Detecting Sensor Bias Faults in Wind Turbine Gearbox Bearing Temperature

Bias sensor faults involve a systematic offset or bias in the sensor measurements. This fault introduces a constant error in the data, leading to inaccuracies in the readings. In the first scenario, we evaluated the monitoring of a sensor bias fault in the Gearbox bearing temperature (Gb2t) variable using the proposed DICA-DEWMA schemes. Detecting bias sensor faults in the Gb2t variable is of critical importance in wind turbine monitoring and maintenance. The Gearbox bearing temperature is a crucial parameter that reflects the health and performance of the gearbox system, which is a vital component in wind turbine operations. A bias sensor fault in the Gb2t variable can have significant implications for the overall performance and reliability of the wind turbine. It can lead to inaccurate temperature readings, which may result in incorrect assessments of the gearbox's operating conditions. This can further lead to suboptimal maintenance decisions, increased downtime, and potential damage to the gearbox components. By accurately detecting bias sensor faults in the Gb2t variable, the monitoring system can provide timely alerts and notifications to the operators or maintenance personnel. This enables them to take corrective actions promptly, such as recalibrating or replacing the faulty sensor, ensuring accurate temperature measurements, and preventing any adverse effects on the gearbox's operation. Furthermore, by detecting bias sensor faults, operators and maintenance personnel gain insights into the performance of the sensor network and its reliability. This information can be used to improve the overall sensor calibration and maintenance processes, ensuring the accuracy and integrity of the collected data.

Here, a bias fault was introduced in the Gb2t variable, accounting for 15% of the total variation in that variable. The fault was introduced starting from the sampling time instant 1500 and continued until the end of the testing data. The purpose of this scenario was to assess the capability of the DICA-DEWMA scheme to detect and monitor the presence of a bias sensor fault in the Gb2t variable. By introducing a bias fault, we created an artificial condition where the variable exhibited a consistent and systematic shift from its normal behavior. This allowed us to evaluate the sensitivity and effectiveness of the DICA-DEWMA scheme in detecting such abnormal behavior. The result plots illustrating the performance of ICA and DICA-based indicators in detecting the bias fault are shown in Figures 2 and 3.

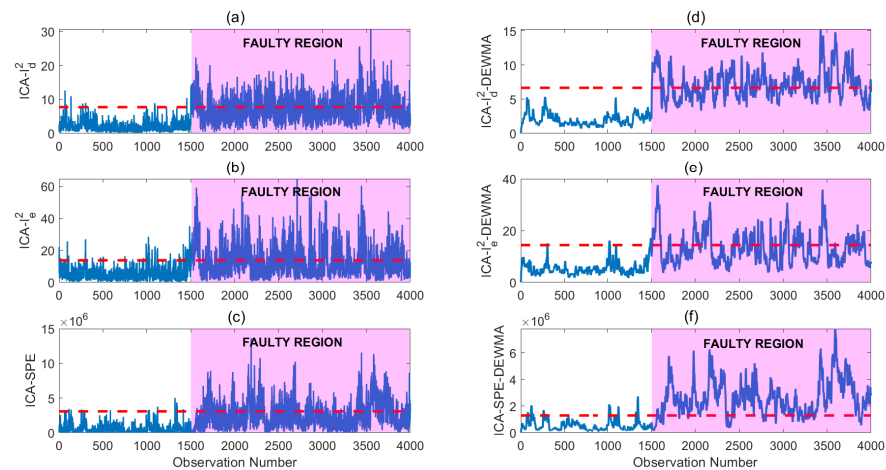


**Figure 2.** Illustration of the performance of the ICA-based indicators in monitoring a bias fault: (a)  $ICA-I_d^2$ , (b)  $ICA-I_e^2$ , (c)  $ICA-SPE$ , (d)  $ICA-I_d^2-DEWMA$ , (e)  $ICA-I_e^2-DEWMA$ , and (f)  $ICA-SPE-DEWMA$ .

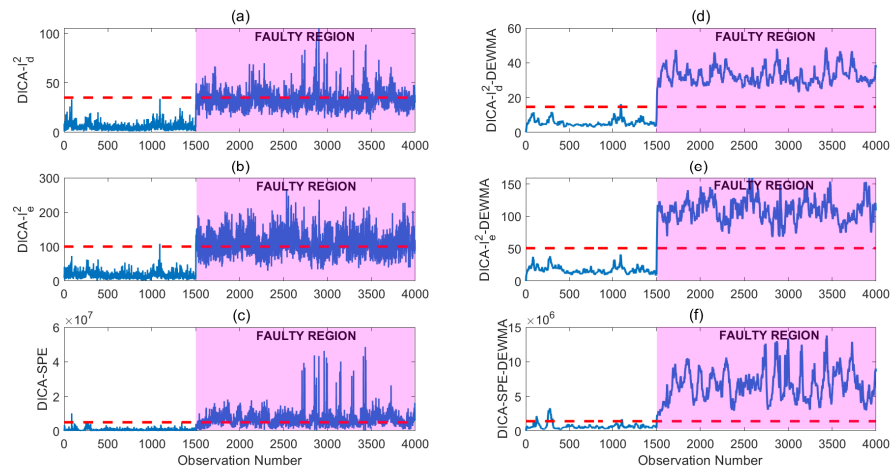


**Figure 3.** Illustration of the performance of the DICA-based indicators in monitoring a bias fault: (a)  $DICA-I_d^2$ , (b)  $DICA-I_e^2$ , (c)  $DICA-SPE$ , (d)  $DICA-I_d^2-DEWMA$ , (e)  $DICA-I_e^2-DEWMA$ , and (f)  $DICA-SPE-DEWMA$ .

Upon visual inspection, it is evident that the conventional ICA indicators exhibit limitations in accurately identifying the fault. These indicators demonstrate a high number of missed detections and few false alarms, as observed in the plots (Figure 2a–c). On the other hand, the ICA-DEWMA method performs relatively better in identifying the fault, but some missed detections are still noticeable within the fault region (Figure 2d–f). In contrast, the DICA-based DEWMA indicators exhibit improved detection performance with minimal false alarms. Comparatively, the DICA-DEWMA strategy outperforms all other indicators in terms of fault detection within the fault region, as depicted in Figure 3d–f. The DICA-DEWMA schemes provide enhanced sensitivity and accuracy in identifying the bias fault, resulting in a more reliable and precise fault detection capability.

The performance of various fault detection schemes in monitoring the bias fault is presented in Table 5. Results in Table 5 show that the PCA and PCA-DEWMA-based schemes exhibit poor performance, as indicated by their low F1-score values. These schemes fail to accurately detect the presence of the fault and also generate a few false alarms. On the other hand, the DPCA and DPCA-DEWMA-based schemes show slightly better performance with higher detection rates and F1-score values. The ICA and ICA-DEWMA-based schemes also struggle to identify the bias fault accurately, as shown by their F1-score values of 36.11%, 50.67%, 60.43%, 58.91%, 47.03%, and 89.81%.

**Table 5.** Detection results of the investigated detectors in the presence of sensor bias faults in wind turbine gearbox bearing temperature.

Method	FPR	TPR	Precision	Recall	F1-Score
PCA- $T^2$	10.40	30.92	83.92	30.92	45.00
PCA-SPE	1.60	16.48	94.40	16.48	27.80
PCA- $T^2$ -DEWMA	7.13	32.16	88.20	32.16	47.23
PCA-SPE-DEWMA	0.85	24.75	98.00	24.75	39.50
DPCA- $T^2$	5.00	68.23	95.70	68.23	79.60
DPCA-SPE	0.00	49.50	100.00	49.50	66.00
DPCA- $T^2$ -DEWMA	2.73	75.45	97.87	75.45	85.30
DPCA-SPE-DEWMA	0.00	60.48	100.00	60.48	75.37
ICA- $I_d^2$	0.15	22.15	99.40	22.15	36.11
ICA- $I_e^2$	0.10	34.38	99.50	34.38	50.67
ICA-SPE	0.35	43.75	99.40	43.75	60.43
ICA-DEWMA- $I_d^2$	0.00	41.76	100.00	41.76	58.91
ICA-DEWMA- $I_e^2$	0.00	30.75	100.00	30.75	47.03
ICA-DEWMA-SPE	2.45	81.44	99.80	81.44	89.81
DICA- $I_d^2$	0.00	40.75	100.00	40.75	57.90
DICA- $I_e^2$	0.00	42.45	100.00	42.45	59.55
DICA-SPE	0.32	60.15	98.00	60.15	74.73
DICA-DEWMA- $I_d^2$	0.00	100.00	100.00	100.00	100.00
DICA-DEWMA- $I_e^2$	0.00	100.00	100.00	100.00	100.00
DICA-DEWMA-SPE	0.85	100.00	99.50	100.00	99.74

Although the DICA-based schemes perform better than the conventional ICA-based schemes with no false alarms and improved detection rates, the fault detection is still not as precise as desired for an effective fault detection strategy. In contrast, the proposed DICA-DEWMA-based schemes outperform other methods for identifying the bias fault accurately. These schemes achieve excellent F1-score values of 100%, 100%, and 99.74%, respectively, indicating their superior performance compared to other schemes (Table 5). Overall, the results emphasize the effectiveness of the DICA-DEWMA schemes in detecting and monitoring a bias sensor fault in the Gearbox bearing temperature variable, outperforming other evaluated schemes.

#### 4.2.2. Detecting Precision Degradation Sensor Faults in Wind Turbine Generator Bearing Temperature

Degradation sensor fault represents a scenario where a sensor's performance deteriorates gradually over time, leading to reduced accuracy and precision in the measurements. This type of fault can occur due to wear and tear, aging, or calibration drift in the sensor. In this case study, we aim to assess the effectiveness of the proposed approach in detecting sensor precision degradation faults, specifically in the Generator bearing temperature variable (Db1t). Detecting sensor precision degradation faults in the Db1t variable is critical in ensuring the reliable and accurate operation of the monitoring wind turbine. The Db1t is a crucial variable that provides insights into the health and performance of the generator bearing, which is a key component in the power generation of wind turbines. A sensor precision degradation fault in this variable refers to a gradual decline in the accuracy of the sensor measurements over time. This fault can occur due to various factors such as aging, wear, and tear, environmental conditions, or calibration issues. When the sensor's precision degrades, the measurements it provides become less accurate, leading to potential inaccuracies in fault detection and decision-making processes.

By introducing a precision degradation fault in the Db1t variable, we simulate a scenario where the sensor's accuracy gradually diminishes between the sampling time instants 2000 and 4000 of the testing data. This allows us to evaluate the ability of the proposed

approach to identify and monitor such degradation. To provide a comprehensive understanding, the detection performance of the ICA, ICA-DEWMA, DICA, and DICA-DEWMA based indicators is visually represented through time-series graphs in Figures 4 and 5. These graphs illustrate the behavior of the different schemes in detecting the precision degradation fault. While the ICA-based schemes exhibit the ability to detect the fault with a slight delay, the DICA-DEWMA-based scheme demonstrates an advantage by detecting the fault earlier than the other schemes.

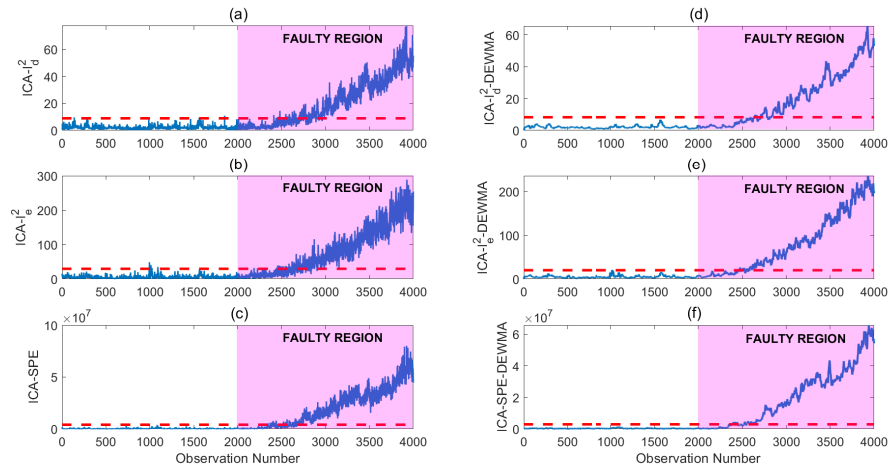


**Figure 4.** Detection performance of the ICA-based indicators in the presence of precision degradation sensor fault in wind turbine generator bearing temperature: (a)  $ICA-I_d^2$ , (b)  $ICA-I_e^2$ , (c) ICA-SPE, (d)  $ICA-I_d^2$ -DEWMA, (e)  $ICA-I_e^2$ -DEWMA, and (f) ICA-SPE-DEWMA.

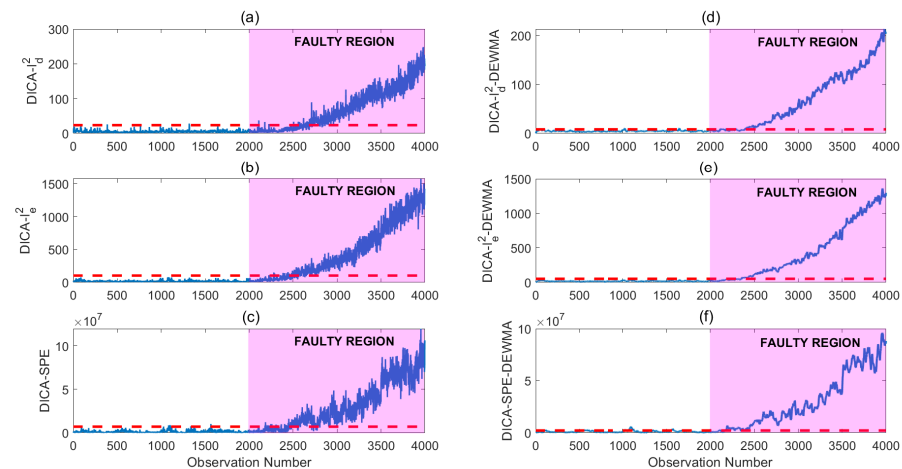


**Figure 5.** Detection performance of the DICA-based indicators in the presence of precision degradation sensor fault in wind turbine generator bearing temperature: (a)  $DICA-I_d^2$ , (b)  $DICA-I_e^2$ , (c) DICA-SPE, (d)  $DICA-I_d^2$ -DEWMA, (e)  $DICA-I_e^2$ -DEWMA, and (f) DICA-SPE-DEWMA.

The evaluation results are summarized in Table 6, which compares the detection performance of various fault detection schemes. It is observed that the PCA- $T^2$  and PCA- $T^2$ -DEWMA schemes exhibit high false alarm rates and relatively lower detection rates compared to other methods. On the contrary, the remaining schemes demonstrate satisfactory detection of the precision degradation fault, as indicated by their favorable F1-score values in the table. Of particular interest is the superior performance of the DICA-DEWMA scheme among the evaluated approaches. It achieves improved F1-scores of 91.30%, 92%, and 94%, respectively, indicating its effectiveness in detecting and monitoring the precision degradation fault. This performance enhancement can be attributed to combining the DICA technique, which captures process dynamics more accurately by

incorporating historical data, and the DEWMA approach, which applies a moving average scheme to conventional statistics for improved fault detection.

**Table 6.** Detection results of the investigated detectors in the presence of precision degradation sensor fault in wind turbine generator bearing temperature.

Method	FPR	TPR	Precision	Recall	F1-Score
PCA- $T^2$	9.70	40.90	80.00	40.90	54.12
PCA-SPE	0.15	72.55	99.65	72.55	84.00
PCA- $T^2$ -DEWMA	8.45	46.85	84.71	46.85	60.59
PCA-SPE-DEWMA	0.00	75.40	100.00	75.40	85.97
DPCA- $T^2$	5.10	66.72	92.90	66.72	77.90
DPCA-SPE	0.00	76.28	100.00	76.28	86.50
DPCA- $T^2$ -DEWMA	2.05	69.37	97.10	69.37	80.50
DPCA-SPE-DEWMA	0.00	77.87	100.00	77.87	87.51
ICA- $I_d^2$	0.00	62.75	100.00	62.75	77.14
ICA- $I_e^2$	1.15	64.85	99.15	64.85	78.60
ICA-SPE	0.75	78.68	99.70	78.68	88.10
ICA-DEWMA- $I_d^2$	0.00	67.25	100.00	58.00	73.00
ICA-DEWMA- $I_e^2$	0.00	70.00	100.00	70.00	82.35
ICA-DEWMA-SPE	0.00	84.33	100.00	84.33	91.49
DICA- $I_d^2$	0.00	69.50	100.00	69.50	82.22
DICA- $I_e^2$	0.00	75.75	100.00	75.75	86.20
DICA-SPE	0.00	83.25	100.00	83.25	90.80
DICA-DEWMA- $I_d^2$	0.00	84.00	100.00	84.00	91.30
DICA-DEWMA- $I_e^2$	0.00	85.15	100.00	85.15	92.00
DICA-DEWMA-SPE	0.00	88.75	100.00	88.75	94.00

Overall, evaluating the proposed approach for detecting sensor precision degradation faults in the  $Dbt$  variable highlights its effectiveness and superiority over other fault detection schemes. By incorporating historical data and applying the DEWMA technique, the DICA-DEWMA scheme demonstrates improved detection performance.

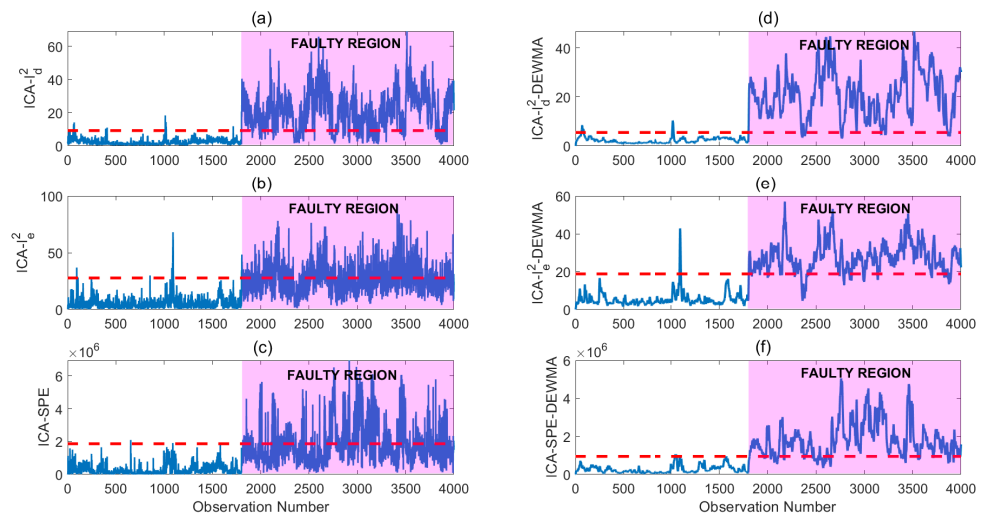
#### 4.2.3. Freezing Sensor Fault Detection in Wind Turbine Anemometer

Freezing sensor fault represents a scenario where a sensor becomes stuck at a particular reading and fails to update its measurements. It simulates situations where sensor data becomes stagnant or unresponsive. In this case study, we focus on monitoring freeze faults using the proposed DICA-DEWMA scheme. Detecting freezing sensor faults in the anemometer on the nacelle of a wind turbine is crucial for accurate wind measurement, turbine performance optimization, and overall operational efficiency. These faults can lead to inaccurate wind data, compromising turbine control and energy production. Continuous monitoring of sensor performance contributes to overall system health and long-term reliability. Overall, detecting freezing sensor faults is essential for safe and efficient wind turbine operation, enabling operators to maximize energy production and minimize costs.

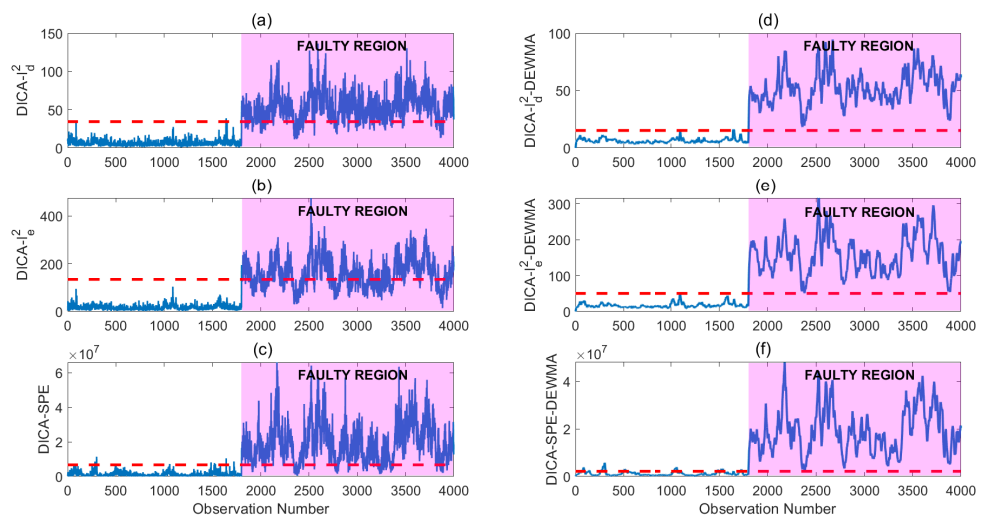
Here, a freeze fault is introduced in variable  $Ws1$ , where the temperature value remains at 77.7 degrees between sampling time instants 2000 and 4000 of the testing data. The goal is to evaluate the performance of different fault detection methods in identifying this freeze fault. To provide a visual representation of the detection performance, Figures 6 and 7 present the time-series graphs of the ICA, ICA-DEWMA, DICA, and DICA-DEWMA-based indicators. These graphs depict the evolution of fault indicators over time. Notably, Figure 7d–f highlights the superiority of the proposed DICA-DEWMA fault detection scheme over other methods in terms of fault detection.

Table 7 provides an overview of the performance of various methods in detecting the freeze fault. The PCA- $T^2$  and PCA- $T^2$ -DEWMA schemes show lower F1-score values, indicating more false alarms than other methods. On the other hand, the DPCA-DEWMA,

ICA, ICA-DEWMA, and DICA-based schemes exhibit better identification of the freeze fault, as shown by their higher F1-score values. However, none of the methods can completely detect the sensor fault. The DICA-based DEWMA schemes demonstrate higher F1-score values due to the sensitivity of the DEWMA scheme in detecting small changes. This makes the DICA-DEWMA scheme more robust than other methods, improving its performance in identifying the freeze fault.



**Figure 6.** Illustration of the performance of the ICA-based indicators in monitoring a freezing fault: (a)  $ICA-I_d^2$ , (b)  $ICA-I_e^2$ , (c)  $ICA-SPE$ , (d)  $ICA-I_d^2-DEWMA$ , (e)  $ICA-I_e^2-DEWMA$ , and (f)  $ICA-SPE-DEWMA$ .



**Figure 7.** Illustration of the performance of the DICA-based indicators in monitoring a freezing fault: (a)  $DICA-I_d^2$ , (b)  $DICA-I_e^2$ , (c)  $DICA-SPE$ , (d)  $DICA-I_d^2-DEWMA$ , (e)  $DICA-I_e^2-DEWMA$ , and (f)  $DICA-SPE-DEWMA$ .

#### 4.2.4. Detecting Sensor Bias Faults in Wind Turbine Generator Speed

This scenario focuses on monitoring sensor bias faults in wind turbine generator speed. Bias faults are commonly observed in wind turbines and can significantly impact their performance. The speed of the generator directly affects the power generation capability and overall performance of the turbine. A bias fault in the speed sensor can lead to inaccurate measurements, causing deviations in the actual generator speed. This can result in suboptimal turbine operation, reduced energy output, and potential mechanical

stress on the turbine components. By detecting and monitoring sensor bias faults, it is possible to identify deviations from the expected speed behavior and take corrective actions promptly. This helps maintain the turbine's operational integrity, optimize power generation, and minimize the risk of costly failures or downtime. Additionally, accurate speed measurements are essential for effectively controlling and coordinating wind turbine arrays, ensuring grid stability and efficient power integration. Therefore, detecting sensor bias faults in wind turbine Generator speed is crucial in enhancing turbine performance, reliability, and overall wind energy production.

**Table 7.** Detection results in the presence of a freezing sensor in wind turbine anemometer.

Method	FPR	TPR	Precision	Recall	F1-Score
PCA- $T^2$	11.83	38.23	79.86	38.23	51.74
PCA-SPE	0.23	76.36	99.70	76.36	86.51
PCA- $T^2$ -DEWMA	9.50	39.73	83.63	39.73	53.55
PCA-SPE-DEWMA	0.00	80.76	100.00	80.76	89.41
DPCA- $T^2$	6.25	43.84	89.55	43.84	59.03
DPCA-SPE	1.40	77.75	98.50	77.75	87.04
DPCA- $T^2$ -DEWMA	0.60	46.40	99.00	46.40	62.90
DPCA-SPE-DEWMA	0.00	82.63	10.00	82.63	90.40
ICA- $I_d^2$	2.13	92.45	98.54	92.45	95.39
ICA- $I_c^2$	1.45	60.70	99.06	60.70	75.10
ICA-SPE	0.32	69.88	99.60	69.88	82.36
ICA-DEWMA- $I_d^2$	1.23	97.25	99.00	97.25	98.24
ICA-DEWMA- $I_c^2$	1.03	89.70	98.90	89.70	94.12
ICA-DEWMA-SPE	0.12	92.30	99.00	92.30	96.11
DICA- $I_d^2$	0.00	92.12	100.00	92.12	95.89
DICA- $I_c^2$	0.00	71.12	100.00	71.12	83.12
DICA-SPE	1.12	88.34	99.00	88.34	93.54
DICA-DEWMA- $I_d^2$	0.00	100.00	100.00	100.00	100.00
DICA-DEWMA- $I_c^2$	0.00	100.00	100.00	100.00	100.00
DICA-DEWMA-SPE	0.40	99.75	99.70	99.75	99.90

Here, we analyze the bias fault in the generator variable  $D_s$ , which occurs at the sampling time instant 1000 and diminishes at 3200. Figures 8 and 9 show the detection results of the investigated monitoring ICA and DICA-based fault detection methods.

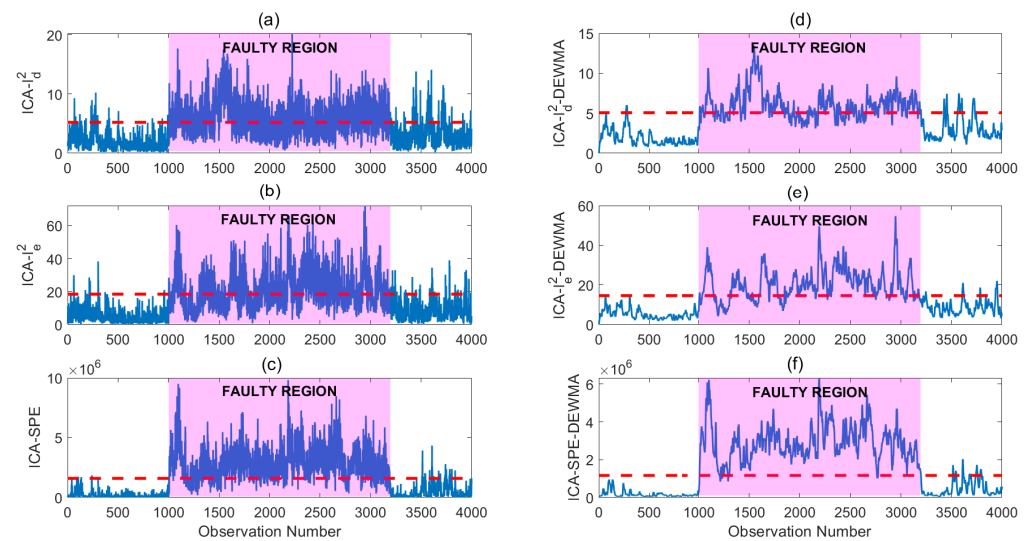


**Figure 8.** Illustration of the performance of the ICA-based indicators in monitoring bias fault in turbine generator speed: (a)  $ICA-I_d^2$ , (b)  $ICA-I_e^2$ , (c)  $ICA-SPE$ , (d)  $ICA-I_d^2-DEWMA$ , (e)  $ICA-I_e^2-DEWMA$ , and (f)  $ICA-SPE-DEWMA$ .

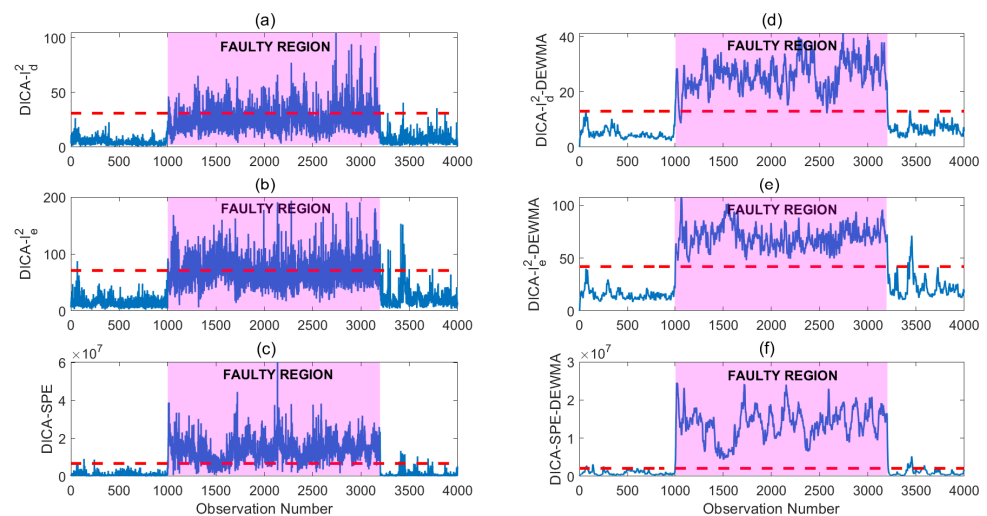


**Figure 9.** Illustration of the performance of the DICA-based indicators in monitoring bias fault in turbine generator speed: (a)  $DICA-I_d^2$ , (b)  $DICA-I_e^2$ , (c)  $DICA-SPE$ , (d)  $DICA-I_d^2-DEWMA$ , (e)  $DICA-I_e^2-DEWMA$ , and (f)  $DICA-SPE-DEWMA$ .

Table 8 provides a comprehensive summary of the performance of various methods based on these metrics. The  $T^2$  fault indicator in PCA and DPCA-based schemes exhibit a high FAR and low FDR, leading to low F1-score values. On the other hand, the SPE indicator in PCA and DPCA-based schemes demonstrate a low FAR and improved FDR compared to the  $T^2$  indicator, but it still falls short in providing effective fault detection.

**Table 8.** Detection results in the presence of a bias sensor fault in the wind turbine generator speed.

Method	FPR	TPR	Precision	Recall	F1-Score
PCA- $T^2$	20.17	27.14	62.18	27.14	37.70
PCA-SPE	0.00	47.68	100.00	47.68	64.57
PCA- $T^2$ -DEWMA	18.37	29.68	66.30	29.78	41.05
PCA-SPE-DEWMA	0.00	50.27	100.00	50.27	66.90
DPCA- $T^2$	12.56	30.27	74.60	30.27	43.01
DPCA-SPE	0.72	38.82	98.61	38.82	55.80
DPCA- $T^2$ -DEWMA	18.06	48.75	76.60	48.75	59.38
DPCA-SPE-DEWMA	0.00	68.59	100.00	68.59	81.39
ICA- $I_d^2$	0.98	24.75	97.00	24.75	39.70
ICA- $I_e^2$	2.75	33.85	93.71	33.85	49.90
ICA-SPE	2.85	91.75	97.40	91.75	94.90
ICA-DEWMA- $I_d^2$	0.45	41.21	99.12	41.21	57.93
ICA-DEWMA- $I_e^2$	0.73	74.27	99.26	74.27	84.73
ICA-DEWMA-SPE	3.45	99.75	97.30	99.75	99.63
DICA- $I_d^2$	0.12	38.35	99.76	38.35	56.44
DICA- $I_e^2$	2.85	41.45	94.50	41.45	58.03
DICA-SPE	1.45	94.50	98.76	94.50	96.60
DICA-DEWMA- $I_d^2$	0.00	99.75	100.00	99.75	99.87
DICA-DEWMA- $I_e^2$	0.75	100.00	99.41	100.00	99.70
DICA-DEWMA-SPE	0.45	100.00	99.73	100.00	99.81

#### 4.2.5. Detecting Sensor Precision Degradation Fault in Wind Turbine Generator Speed

In this last experiment, we focus on the detection of sensor precision degradation faults in the Generator Speed (Ds) variable using the proposed DICA-DEWMA approach. The accurate monitoring of sensor precision degradation in Ds is crucial for maintaining the reliable and efficient operation of wind turbines. By identifying and addressing these faults promptly, potential performance issues and costly downtime can be mitigated, ensuring optimal turbine performance and prolonging the lifespan of the equipment. This fault gradually diminishes between the sampling time instants 2000 and 4000 of the testing data. Table 9 summarizes the obtained detection results by the investigated PCA, ICA, DPCA, and DICA-based monitoring methods. We observe that DICA-based DEWMA schemes outperformed the other methods in detecting this sensor precision degradation fault with better F1-score value as compared to the other methods.

**Table 9.** Detection results in the presence of sensor precision degradation faults in the generator speed.

Method	FPR	TPR	Precision	Recall	F1-Score
PCA- $T^2$	4.50	67.95	94.40	67.95	79.19
PCA-SPE	0.00	51.35	100.00	51.35	67.80
PCA- $T^2$ -DEWMA	2.55	68.83	96.15	68.83	80.21
PCA-SPE-DEWMA	0.00	53.60	100.00	53.60	69.79
DPCA- $T^2$	2.05	69.35	97.12	69.35	80.66
DPCA-SPE	0.00	55.66	100.00	55.66	71.26
DPCA- $T^2$ -DEWMA	0.30	71.57	99.61	71.57	83.30
DPCA-SPE-DEWMA	0.00	59.61	100.00	59.61	74.69
ICA- $I_d^2$	0.85	56.65	98.52	56.65	72.01
ICA- $I_e^2$	0.65	60.70	98.85	60.70	75.95
ICA-SPE	0.70	56.45	98.77	56.45	71.02
ICA-DEWMA- $I_d^2$	0.30	59.05	99.57	59.05	73.95
ICA-DEWMA- $I_e^2$	0.00	62.75	100.00	62.75	77.11
ICA-DEWMA-SPE	0.00	58.95	100.00	58.95	74.17
DICA- $I_d^2$	0.00	77.32	100.00	77.32	87.20
DICA- $I_e^2$	0.00	64.27	100.00	64.27	78.24
DICA-SPE	0.03	61.35	99.00	61.35	76.14
DICA-DEWMA- $I_d^2$	0.01	80.00	99.00	80.00	88.50
DICA-DEWMA- $I_e^2$	0.00	81.45	100.00	81.45	89.77
DICA-DEWMA-SPE	0.02	82.35	99.25	82.35	90.31

## 5. Conclusions

This paper presents a novel semi-supervised monitoring technique for fault identification in wind turbines using SCADA data. This approach has demonstrated superior performance by leveraging the advantages of DICA, fault indicators, and the DEWMA chart compared to traditional PCA- and ICA-based methods. The integration of DICA allows for capturing the temporal dynamics and dependencies in the data, improving the modeling and detection capabilities. Furthermore, incorporating fault indicators and the DEWMA chart enhances the sensitivity of fault detection, making it capable of detecting even small sensor faults in wind turbines. Through extensive experimentation with various sensor faults in wind turbine data, it has been shown that our proposed technique achieves high detection rates and reduces false alarm rates. This highlights its effectiveness in accurately identifying faults, enabling timely maintenance interventions, and minimizing downtime. One of the key advantages of this approach is its reliance solely on SCADA data, eliminating the need for additional sensors or equipment. This makes it a practical and cost-effective solution for wind turbine monitoring, as it utilizes the available data without incurring additional expenses.

In terms of future directions, there are several avenues for further research and development in the field of fault detection for wind turbines. Firstly, integrating advanced machine learning techniques, such as deep learning, recurrent neural networks (RNNs), or long short-term memory (LSTM) networks, can be explored to enhance fault detection capabilities. These techniques can potentially capture complex patterns and dependencies in the data, thereby improving the accuracy and robustness of the fault detection system [52]. Second, the concept of multimodal data fusion can be investigated. Wind turbines generate data from various sensors, including vibration, temperature, and acoustic sensors. Integrating data from multiple modalities can provide a more comprehensive understanding of the system's health. Future research can focus on developing multimodal data fusion techniques to leverage the complementary information from different sensor types, enhancing the accuracy and reliability of fault detection. Additionally, future work can explore the integration of online fault diagnosis and prognosis capabilities into the proposed technique. By continuously monitoring the system and analyzing real-time data, the technique can detect faults and provide information about fault severity, remaining

useful life, and appropriate maintenance actions. This proactive approach can improve decision-making and maintenance strategies. Furthermore, incorporating external data sources, such as weather conditions, grid parameters, and turbine operation logs, can enhance fault detection. Considering the influence of external factors can improve the understanding of the system's behavior in different operating conditions and enhance the fault detection capabilities. To ensure the generalizability and robustness of the approach, future research should validate the proposed technique on larger and more diverse datasets from different wind turbine models and operating environments. Finally, the aspect of explainability and interpretability should be considered. As fault detection techniques become more complex, providing clear explanations and insights into the detected faults becomes essential. Developing methodologies to enhance interpretability and explainability will enable operators and maintenance personnel to understand the reasoning behind the identified anomalies and make informed decisions.

**Author Contributions:** K.R.K., conceptualization, formal analysis, investigation, methodology, software, writing—original draft, and writing—review and editing. F.H., conceptualization, formal analysis, investigation, methodology, software, supervision, writing—original draft, and writing—review and editing. M.M., conceptualization, formal analysis, investigation, methodology, software, supervision, writing—original draft, and writing—review and editing. Y.S., investigation, methodology, conceptualization, supervision, and writing—review and editing. All authors have read and agreed to the published version of the manuscript.

**Funding:** This publication is based upon work supported by King Abdullah University of Science and Technology (KAUST) Research Funding (KRF) from the Climate and Livability Initiative (CLI) under Award No. ORA-2022-5339.

**Institutional Review Board Statement:** Not applicable.

**Informed Consent Statement:** Not applicable.

**Data Availability Statement:** Not applicable.

**Conflicts of Interest:** The authors declare no conflict of interest.

## References

1. Harrou, F.; Sun, Y.; Dairi, A.; Taghezouit, B.; Khadraoui, S. Advanced data-driven methods for monitoring solar and wind energy systems. *Front. Energy Res.* **2023**, *11*, 1147746. [[CrossRef](#)]
2. Kou, L.; Li, Y.; Zhang, F.; Gong, X.; Hu, Y.; Yuan, Q.; Ke, W. Review on Monitoring, Operation and Maintenance of Smart Offshore Wind Farms. *Sensors* **2022**, *22*, 2822. [[CrossRef](#)]
3. McKenna, R.; Pfenninger, S.; Heinrichs, H.; Schmidt, J.; Staffell, I.; Bauer, C.; Gruber, K.; Hahmann, A.N.; Jansen, M.; Klingler, M.; et al. High-resolution large-scale onshore wind energy assessments: A review of potential definitions, methodologies and future research needs. *Renew. Energy* **2022**, *182*, 659–684. [[CrossRef](#)]
4. Hanifi, S.; Liu, X.; Lin, Z.; Lotfian, S. A critical review of wind power forecasting methods—Past, present and future. *Energies* **2020**, *13*, 3764. [[CrossRef](#)]
5. Sawant, M.; Thakare, S.; Rao, A.P.; Feijóo-Lorenzo, A.E.; Bokde, N.D. A review on state-of-the-art reviews in wind-turbine-and wind-farm-related topics. *Energies* **2021**, *14*, 2041. [[CrossRef](#)]
6. Anand, H.; Ramasubbu, R. Dynamic economic emission dispatch problem with renewable integration focusing on deficit scenario in India. *Int. J. Bio Inspired Comput.* **2020**, *15*, 63–73. [[CrossRef](#)]
7. Elgendi, M.; AlMallahi, M.; Abdelkhalig, A.; Selim, M.Y. A review of wind turbines in complex terrain. *Int. J. Thermofluids* **2023**, *17*, 100289. [[CrossRef](#)]
8. Qiao, W.; Lu, D. A survey on wind turbine condition monitoring and fault diagnosis—Part II: Signals and signal processing methods. *IEEE Trans. Ind. Electron.* **2015**, *62*, 6546–6557. [[CrossRef](#)]
9. Jonas, S.; Anagnostos, D.; Brodbeck, B.; Meyer, A. Vibration fault detection in wind turbines based on normal behaviour models without feature engineering. *Energies* **2023**, *16*, 1760. [[CrossRef](#)]
10. Teng, W.; Ding, X.; Tang, S.; Xu, J.; Shi, B.; Liu, Y. Vibration analysis for fault detection of wind turbine drivetrains—A comprehensive investigation. *Sensors* **2021**, *21*, 1686. [[CrossRef](#)]
11. Liu, Z.; Wang, X.; Zhang, L. Fault diagnosis of industrial wind turbine blade bearing using acoustic emission analysis. *IEEE Trans. Instrum. Meas.* **2020**, *69*, 6630–6639. [[CrossRef](#)]
12. Mollasalehi, E.; Wood, D.; Sun, Q. Indicative fault diagnosis of wind turbine generator bearings using tower sound and vibration. *Energies* **2017**, *10*, 1853. [[CrossRef](#)]

13. Astolfi, D.; Scappaticci, L.; Terzi, L. Fault diagnosis of wind turbine gearboxes through temperature and vibration data. *Int. J. Renew. Energy Res.* **2017**, *7*, 965–976.
14. Harrou, F.; Saidi, A.; Sun, Y. Wind power prediction using bootstrap aggregating trees approach to enabling sustainable wind power integration in a smart grid. *Energy Convers. Manag.* **2019**, *201*, 112077. [[CrossRef](#)]
15. Zaher, A.; McArthur, S.; Infield, D.; Patel, Y. Online wind turbine fault detection through automated SCADA data analysis. *Wind. Energy Int. J. Prog. Appl. Wind. Power Convers. Technol.* **2009**, *12*, 574–593. [[CrossRef](#)]
16. Dao, P.B.; Staszewski, W.J.; Barszcz, T.; Uhl, T. Condition monitoring and fault detection in wind turbines based on cointegration analysis of SCADA data. *Renew. Energy* **2018**, *116*, 107–122. [[CrossRef](#)]
17. Dao, P.B. Condition monitoring and fault diagnosis of wind turbines based on structural break detection in SCADA data. *Renew. Energy* **2022**, *185*, 641–654. [[CrossRef](#)]
18. Dao, P.B. On Cointegration Analysis for Condition Monitoring and Fault Detection of Wind Turbines Using SCADA Data. *Energies* **2023**, *16*, 2352. [[CrossRef](#)]
19. Stetco, A.; Dinmohammadi, F.; Zhao, X.; Robu, V.; Flynn, D.; Barnes, M.; Keane, J.; Nenadic, G. Machine learning methods for wind turbine condition monitoring: A review. *Renew. Energy* **2019**, *133*, 620–635. [[CrossRef](#)]
20. Hsu, J.Y.; Wang, Y.F.; Lin, K.C.; Chen, M.Y.; Hsu, J.H.Y. Wind turbine fault diagnosis and predictive maintenance through statistical process control and machine learning. *IEEE Access* **2020**, *8*, 23427–23439. [[CrossRef](#)]
21. Du, B.; Narusue, Y.; Furusawa, Y.; Nishihara, N.; Indo, K.; Morikawa, H.; Iida, M. Clustering Wind Turbines for SCADA Data-Based Fault Detection. *IEEE Trans. Sustain. Energy* **2022**, *14*, 442–452. [[CrossRef](#)]
22. Wang, Y.; Ma, X.; Qian, P. Wind turbine fault detection and identification through PCA-based optimal variable selection. *IEEE Trans. Sustain. Energy* **2018**, *9*, 1627–1635. [[CrossRef](#)]
23. Pozo, F.; Vidal, Y.; Salgado, Ó. Wind turbine condition monitoring strategy through multiway PCA and multivariate inference. *Energies* **2018**, *11*, 749. [[CrossRef](#)]
24. Wen, X.; Xu, Z. Wind turbine fault diagnosis based on ReliefF-PCA and DNN. *Expert Syst. Appl.* **2021**, *178*, 115016. [[CrossRef](#)]
25. Yang, H.H.; Huang, M.L.; Lai, C.M.; Jin, J.R. An approach combining data mining and control charts-based model for fault detection in wind turbines. *Renew. Energy* **2018**, *115*, 808–816. [[CrossRef](#)]
26. Shao, K.; He, Y.; Liu, X.; Xing, Z.; Du, B. Fault Detection for Wind Turbine System Using Fractional Extended Dispersion Entropy and Cumulative Sum Control Chart. *IEEE Trans. Instrum. Meas.* **2022**, *71*, 1–9. [[CrossRef](#)]
27. Dou, X.; Tan, W.; Chen, S. An Improved Fault Detection Method based on Canonical Variate Analysis for Tricky Faults of Wind Turbine. In Proceedings of the 2020 Chinese Automation Congress (CAC), Shanghai, China, 6–8 November 2020; pp. 4337–4342.
28. Khan, P.W.; Byun, Y.C. A Review of machine learning techniques for wind turbine’s fault detection, diagnosis, and prognosis. *Int. J. Green Energy* **2023**, 1–16. [[CrossRef](#)]
29. Wang, M.H.; Lu, S.D.; Hsieh, C.C.; Hung, C.C. Fault detection of wind turbine blades using multi-channel CNN. *Sustainability* **2022**, *14*, 1781. [[CrossRef](#)]
30. Farrar, N.O.; Ali, M.H.; Dasgupta, D. Artificial intelligence and machine learning in grid connected wind turbine control systems: A comprehensive review. *Energies* **2023**, *16*, 1530. [[CrossRef](#)]
31. Tang, M.; Zhao, Q.; Ding, S.X.; Wu, H.; Li, L.; Long, W.; Huang, B. An improved lightGBM algorithm for online fault detection of wind turbine gearboxes. *Energies* **2020**, *13*, 807. [[CrossRef](#)]
32. Zhang, D.; Qian, L.; Mao, B.; Huang, C.; Huang, B.; Si, Y. A data-driven design for fault detection of wind turbines using random forests and XGboost. *IEEE Access* **2018**, *6*, 21020–21031. [[CrossRef](#)]
33. Xiang, L.; Wang, P.; Yang, X.; Hu, A.; Su, H. Fault detection of wind turbine based on SCADA data analysis using CNN and LSTM with attention mechanism. *Measurement* **2021**, *175*, 109094. [[CrossRef](#)]
34. Kavaz, A.G.; Barutcu, B. Fault detection of wind turbine sensors using artificial neural networks. *J. Sens.* **2018**, *2018*, 5628429. [[CrossRef](#)]
35. Laouti, N.; Othman, S.; Alamir, M.; Sheibat-Othman, N. Combination of model-based observer and support vector machines for fault detection of wind turbines. *Int. J. Autom. Comput.* **2014**, *11*, 274–287. [[CrossRef](#)]
36. Khan, P.W.; Yeun, C.Y.; Byun, Y.C. Fault detection of wind turbines using SCADA data and genetic algorithm-based ensemble learning. *Eng. Fail. Anal.* **2023**, *148*, 107209. [[CrossRef](#)]
37. Li, C.; Zhou, Z.; Wen, C.; Li, Z. Fault Detection of Non-Gaussian and Nonlinear Processes Based on Independent Slow Feature Analysis. *ACS Omega* **2022**, *7*, 6978–6990. [[CrossRef](#)]
38. Lee, J.M.; Yoo, C.; Lee, I.B. Statistical process monitoring with independent component analysis. *J. Process. Control.* **2004**, *14*, 467–485. [[CrossRef](#)]
39. Harrou, F.; Madakyaru, M.; Sun, Y.; Kammammettu, S. Enhanced dynamic data-driven fault detection approach: Application to a two-tank heater system. In Proceedings of the 2017 IEEE Symposium Series on Computational Intelligence (SSCI), Honolulu, HI, USA, 27 November–1 December 2017; pp. 1–6.
40. K, K.R.; Madakyaru, M. Improved Process Monitoring Scheme Using Multi-Scale Independent Component Analysis. *Arab. J. Sci. Eng.* **2022**, *47*, 5985–6000.
41. Ku, W.; Storer, R.H.; Georgakis, C. Disturbance Detection and Isolation by Dynamic Principal Component Analysis. *Chemom. Intell. Lab. Syst.* **1995**, *30*, 179–196. [[CrossRef](#)]

42. Lee, J.M.; Yoo, C.; Lee, I.B. Statistical monitoring of dynamic processes based on dynamic independent component analysis. *Chem. Eng. Sci.* **2004**, *14*, 2995–3006. [[CrossRef](#)]
43. Stefatos, G.; Hamza, B. Dynamic independent component analysis approach for fault detection and diagnosis. *Expert Syst. Appl.* **2010**, *37*, 8606–8617. [[CrossRef](#)]
44. Fan, J.; Wang, Y. Fault detection and diagnosis of non-linear non-Gaussian dynamic processes using kernel dynamic independent component analysis. *Inf. Sci.* **2014**, *259*, 369–379. [[CrossRef](#)]
45. K, K.R.; Madakyaru, M. Performance Evaluation of Independent Component Analysis-Based Fault Detection Using Measurements Corrupted with Noise. *J. Control. Autom. Electr. Syst.* **2021**, *32*, 642–655.
46. Zhang, L.; Chen, G. An extended EWMA mean chart. *Qual. Technol. Quant. Manag.* **2005**, *2*, 39–52. [[CrossRef](#)]
47. Taghezouit, B.; Harrou, F.; Sun, Y.; Arab, A.H.; Larbes, C. A simple and effective detection strategy using double exponential scheme for photovoltaic systems monitoring. *Sol. Energy* **2021**, *214*, 337–354. [[CrossRef](#)]
48. Parzen, E. On estimation of a probability density function and mode. *Ann. Math. Stat.* **1962**, *33*, 1065–1076. [[CrossRef](#)]
49. Ledl, T. Kernel density estimation: Theory and application in discriminant analysis. *Austrian J. Stat.* **2004**, *33*, 267–279. [[CrossRef](#)]
50. Harrou, F.; Saidi, A.; Sun, Y.; Khadraoui, S. Monitoring of photovoltaic systems using improved kernel-based learning schemes. *IEEE J. Photovoltaics* **2021**, *11*, 806–818. [[CrossRef](#)]
51. Harrou, F.; Kadri, F.; Khadraoui, S.; Sun, Y. Ozone measurements monitoring using data-based approach. *Process. Saf. Environ. Prot.* **2016**, *100*, 220–231. [[CrossRef](#)]
52. Harrou, F.; Sun, Y.; Hering, A.S.; Madakyaru, M.; Dairi, A. *Statistical Process Monitoring Using Advanced Data-Driven and Deep Learning Approaches: Theory and Practical Applications*; Elsevier: Amsterdam, The Netherlands, 2020.

**Disclaimer/Publisher’s Note:** The statements, opinions and data contained in all publications are solely those of the individual author(s) and contributor(s) and not of MDPI and/or the editor(s). MDPI and/or the editor(s) disclaim responsibility for any injury to people or property resulting from any ideas, methods, instructions or products referred to in the content.